Japanese Journal of Applied Physics **57**, 116702 (2018)
https://doi.org/10.7567/JJAP.57.116702

REGULAR PAPER

Factors affecting the co-axial electrospraying of core–shell-structured poly(D,L-lactide-*co*-glycolide) microparticles

Demei Lee[1], Ming-Yih Hsu[1,2], Min-Jhan Li[1], Yen-Wei Liu[1], Shih-Jung Liu[1,3*], Cheng-Ying Liu[4], and Hiroshi Ito[4]

[1]*Department of Mechanical Engineering, Chang Gung University, Taoyuan 33302, Taiwan*
[2]*Department of Medical Imaging and Intervention, Chang Gung Memorial Hospital-Linkou, Taoyuan 33305, Taiwan*
[3]*Department of Orthopedic Surgery, Chang Gung Memorial Hospital-Linkou, Taoyuan 33305, Taiwan*
[4]*Graduate School of Organic Materials Science, Yamagata University, Yonezawa, Yamagata 992-8510, Japan*

*E-mail: shihjung@mail.cgu.edu.tw

Received July 3, 2018; accepted August 5, 2018; published online October 3, 2018

Co-axial electrospraying is a simple and versatile process, achieving liquid atomization through electrical forces, to produce core–shell-structured nano/microparticles. Despite its advantages in terms of preparing particles with sizes ranging from 300–500 μm down to 50–70 nm, the optimization of the co-axial electrospraying process remains a challenge. In this study, we investigated experimentally the effects of processing parameters on the size distribution of co-axially electroprayed poly(D,L-lactide-*co*-glycolide) (PLGA) microparticles. The effects of various parameters, including voltage, flow rate ratio, travel distance, and polymeric concentration, were examined using a factorial experimental design. It was found that the particle size of electrosprayed core–shell microparticles decreases with the voltage and travel distance, and it increases with the flow rate of the solutions and the PLGA concentration in the solutions. Furthermore, to verify the existence of proteins in the co-axially electrosprayed microparticles, PLGA was used as the shell, and recombinant enhanced green fluorescent protein (reGFP) was employed as the core material. Transmission electron microscopy (TEM) and laser scanning confocal microscopy (LSCM) were employed to confirm the core–shell structure of the microparticles. The experimental results demonstrated that under optimum conditions, core–shell-structured microparticles can be successfully prepared using a protein with high activity at the core.

1. Introduction

Electrospraying[1,2] is a simple and versatile technique for the manufacture of micro-[3,4] and nano-[5] particles. It is a process of liquid atomization through electrical forces. In this process, the liquid is compelled out of a capillary tube by a high electric force, thus dispersing into fine drops. Electrospraying systems possess some advantages over conventional mechanical atomization processes in that the drop sizes span from the micrometer order to the nanometer order with an almost monodispersed distribution. Furthermore, owing to the electric charges, the droplets formed are self-scattering; and thus droplet coagulation is minimized. In recent years, electrospraying has been widely employed to produce biodegradable nano-/micro-carriers for drug delivery applications.[6–9] Owing to their small size and geometry, electrosprayed particles are well suited for various medicinal applications by direct injection. The micro-/submicro-sized drug particles generated by electrospray possess increased dissolution rates, and thus increased bioavailability owing to the increased surface area.[3–5] The side-effects of drugs can thus be minimized, as a smaller dosage is enough to obtain the same effect.[6–9]

Core–shell-type nano/micro-particles can also be prepared by co-axial[10–15] or tri-axial[16] electrospraying to encapsulate highly biodegradable protein-based therapeutic agents such as growth factors. It has been shown that co-axial electrospraying increases the encapsulation efficiency of proteins compared with the emulsion method.[17] Despite all these advantages, the optimization of co-axial electrospraying remains as a challenge.

Among various biodegradable polymers, poly(D,L-lactide-*co*-glycolide) (PLGA), is one of the most investigated for biomedical applications. PLGA belongs to a class of hydrolytically biodegradable polymers and has been approved by the Food and Drug Administration (FDA) for human use including implants and drug delivery devices. The material has also been widely used for preparing micro-/nanoparticles owing to its biocompatibility and well-documented property of sustained drug release.[18,19]

In this study we investigated the effects of different processing parameters on the co-axial electrospraying of core–shell-structured biodegradable poly(L-lactide-*co*-glycolic acid) microparticles. To prepare the microparticles, a lab-scale co-axial electrospraying setup was adopted. After electrospraying, the morphology of the sprayed microparticles was observed by scanning electron microscopy (SEM). A factorial experiment was carried out to explore the effects of various parameters on the size distribution of co-axially electrosprayed microparticles. Finally, transmission electron microscopy (TEM) and laser scanning confocal microscopy (LSCM) were also employed to confirm the core–shell structure of the microparticles.

2. Materials and methods

2.1 Fabrication of biodegradable core–shell-structured microparticles

The biodegradable materials used were lactide : glycolide/50 : 50 PLGA purchased from Sigma-Aldrich. The solvent adopted was dichloromethane (DCM), also from Sigma-Aldrich.

Biodegradable microparticles were prepared using the co-axial electrospraying device shown schematically in Fig. 1(a), which consists of a specially designed metallic nozzle with two concentric needles [Fig. 1(b)], a ground electrode, a collection disk, and a high-voltage source. Two separately controlled pumps were connected to the inner and outer inlets of the nozzles, so that the solutions for the core and the shell layer can be transported separately. The sizes of the needles were 18G (1.02 mm) and 22G (0.64 mm) for the delivery of outer and inner solutions, respectively.

Various processing parameters were studied in terms of their effects on the size distribution of co-axially electrosprayed core–shell microparticles: voltage, core–shell layer solution flow rate, travel distance between the needle and the

Table I. Parameters used for co-axial electrospraying of core–shell particles.

Test conditions	Voltage (kV)	Flow rate ratio (mL/h) core:shell	Travel distance (cm)	PLGA concentration (%, w/v)
A_1, A_2, A_3	9, 10, 11	0.1 : 0.6	8	6
A_4, A_5	9	0.1 : 0.8, 0.1 : 1	8	6
A_6, A_7	9	0.1 : 0.6	10, 12	6
A_8, A_9	9	0.1 : 0.6	8	7, 8
B_1, B_2, B_3	9, 10, 11	0.1 : 0.8	10	7
B_4, B_5	10	0.1 : 0.6, 0.1 : 1	10	7
B_6, B_7	10	0.1 : 0.8	8, 12	7
B_8, B_9	10	0.1 : 0.8	10	6, 8
C_1, C_2, C_3	9, 10, 11	0.1 : 1	12	8
C_4, C_5	11	0.1 : 0.6, 0.1 : 0.8	12	8
C_6, C_7	11	0.1 : 1	8, 10	8
C_8, C_9	11	0.1 : 1	12	6, 7

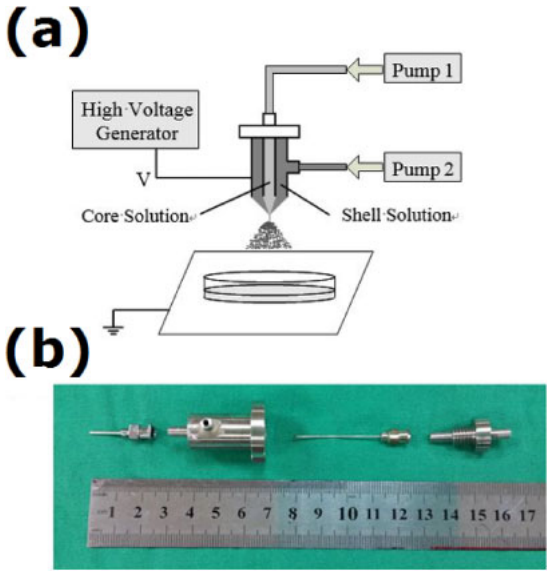

Fig. 1. (Color online) (a) Schematic of the experimental setup for co-axial electrospraying of core–shell microparticles and (b) co-axial nozzle and needles used for the experiments.

collection disk, and PLGA concentration in solutions. Before the experiments, a few test trials were first carried out to determine the ranges of parameters for co-axial electrospraying. At parameters outside the ranges the Taylor cone could not be formed at the needle tip and thus microparticles were not successfully sprayed. The needle was then linked to a high positive DC voltage of either 9, 10, or 11 kV. For the solution for the shell layer, three different weight-to-volume (w/v) percentages were adopted, namely, 6% (360 mg of PLGA dissolved in 6 mL of DCM), 7% (420 mg of PLGA dissolved in 6 mL of DCM), and 8% (480 mg of PLGA dissolved in 6 mL of DCM). On the other hand, 50 μg of recombinant enhanced green fluorescent protein (reGFP; Sigma-Aldrich) dissolved in 1 mL of phosphate-buffered solution was used as the core. Three different core:shell flow rate ratios, namely, 0.1 : 0.6, 0.1 : 0.8, and 0.1 : 1 mL/h, were selected. The travel distance from the needle tip to the collecting disk was set at 8, 10, or 12 cm. Table I shows the processing parameters used in the experiments. After co-axial electrospraying, the size of the core–shell-structured microparticles was measured. By varying one of the parameters in each test (the shaded ones) while keeping the other ones unchanged, we were able to better understand the effects of each parameter on the particle size distribution of electrosprayed microparticles.

2.2 SEM inspection

The morphological structure of electrosprayed microspheres coated with a layer of gold was inspected by field-emission scanning electron microscopy (FESEM; JEOL JSM-7500F). The average microparticle size and size distribution were determined by analyzing SEM images utilizing a commercially available code (ImageJ).

2.3 TEM

Co-axially electrosprayed microspheres deposited on a copper network were observed and inspected by TEM (JEOL JEM-2000EXII).

2.4 LSCM

To verify the existence of proteins inside the microparticles, co-axially electrosprayed microspheres with PLGA as the shell layer and recombinant enhanced reGFP at the core were prepared. After electrospraying, microparticles were deposited above a glass plate. The microparticles were inspected by LSCM (Leica TS SP8X). The wavelength of excitation for reGFP was set at 487 nm.

3. Results and discussion

In this study, experiments were conducted using the lab-scale device equipped with a co-electrospraying nozzle and two concentric needles. Five specimens were used for each test trial.

3.1 Effects of processing parameters on electrosprayed PLGA core–shell-structured microparticles

The effect of voltage applied to the needles and the ground electrode was investigated. Figure 2 shows the co-axially electroprayed PLGA microparticles subjected to voltages of 9, 10, and 11 kV under the processing conditions A1, A2, and A3 shown in Table I, respectively. The size of the microparticles was approximately 17 μm at 9 kV, and decreased with increasing applied voltage. At 11 kV, the microparticle size dropped to about 5 μm.

Figure 3 shows SEM images of core–shell microparticles electrosprayed at various solution flow rates. The solution flow rates under condition C4 were 0.1 and 0.6 mL/h for the core and the shell of co-axially electrosprayed microparticles,

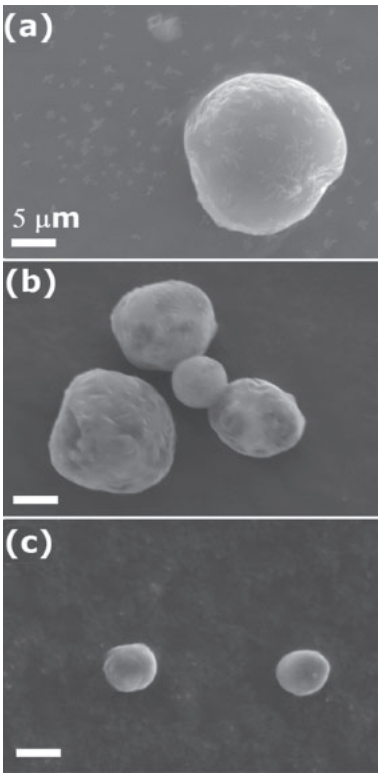

Fig. 2. SEM images of core–shell particles produced under the conditions (a) A1, (b) A2, and (c) A3 in Table I (effect of voltage). Scale bar: 5 μm.

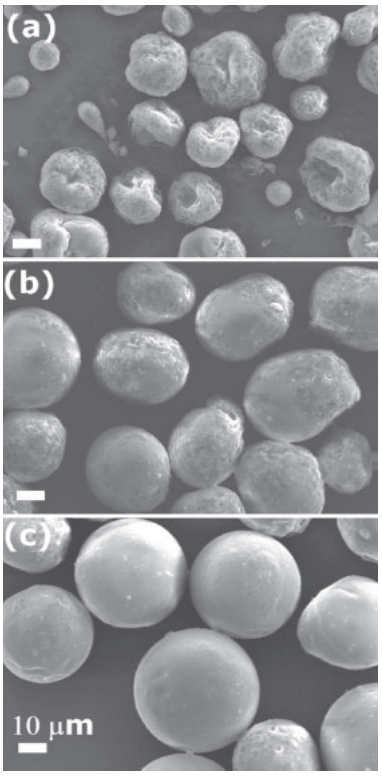

Fig. 3. SEM images of core–shell particles produced under the conditions (a) C4, (b) C5, and (c) C3 in Table I (effect of solution flow rate ratio on particle morphology). Scale bar: 10 μm.

respectively. Meanwhile, the solution flow rate ratios under conditions C5 and C3 were 0.1 : 0.8 and 0.1 : 1 mL/h, respectively. Microparticles prepared at the flow rate ratio of 0.1 : 0.6 mL/h exhibited the smallest size distribution, with

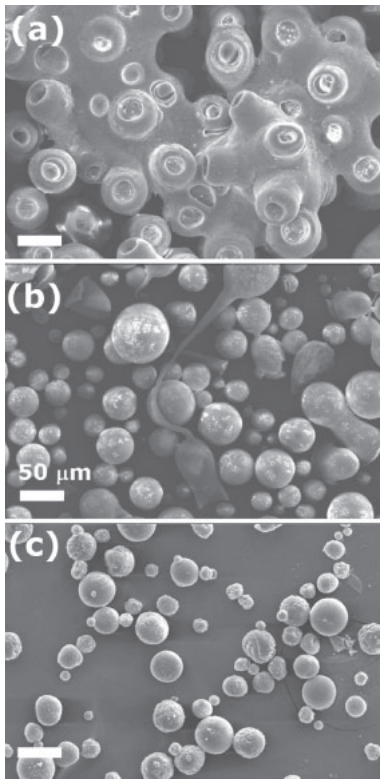

Fig. 4. SEM images of core–shell particles produced under the conditions (a) C6, (b) C7, and (c) C3 in Table I (effect of travel distance). Scale bar: 50 μm.

a broad size distribution ranging from 2 to 15 μm. Sprayed microparticles also exhibited rough surfaces and some with hollowed surfaces. As the flow rate increased, the microparticle size increased and the microparticles showed a more spherical geometry. At the flow rate ratio of 0.1 : 1 mL/h, the obtained microparticles possessed a fairly uniform size distribution at around 40 μm.

The effect of the travel distance between the nozzle to the collection disk on the morphological structure of co-axially electrosprayed PLGA particles was also examined. Figure 4 shows the morphology of the electrosprayed microparticles. The travel distances employed were 8, 10, and 12 cm under conditions C6, C7, and C3 shown in Table I, respectively. The experimental results in Fig. 4 suggest that coalescence occurred when the travel distance of 8 cm was used. As the travel distance was increased, the electrosprayed particles exhibited a transition from coalesced particles to separate smaller particles. When a travel distance of 12 cm was used, the electrosprayed particles showed the smallest particle size distribution, spanning from 5 to 30 μm.

The effect of PLGA concentration in the solutions was studied, and the results are shown in Fig. 5. Three PLGA concentrations were used, namely, 6, 7, and 8% (w/v) under conditions A1, A8, and A9, respectively. When 6% PLGA concentration was employed, electrosprayed particles exhibited rough surfaces. Electrosprayed 7% PLGA particles showed more uniform and smallest size distribution. When 8% PLGA was used, the prepared particles showed a tailed geometry.

3.2 Microparticles prepared using the optimum processing conditions

In this study we investigated the effects of various processing

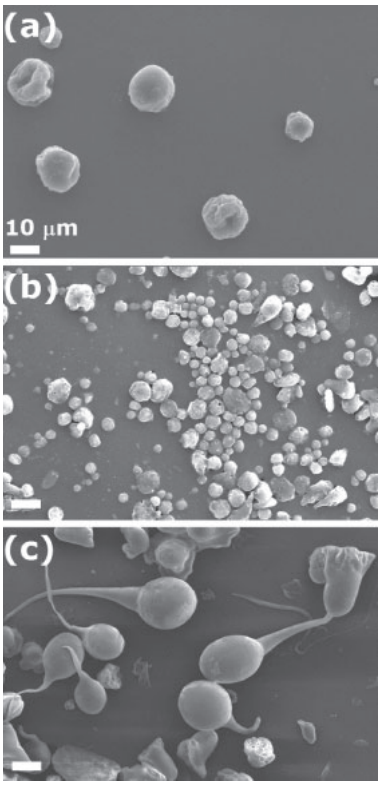

Fig. 5. SEM images of core–shell particles produced under the conditions (a) A1, (b) A8, and (c) A9 in Table I (effect of PLGA concentrations). Scale bar: 10 μm.

parameters on the morphology of electrosprayed core–shell-structured microparticles. On the basis of the experimental results, three optimum sets of processing parameters were selected to fabricate the core–shell-structured PLGA microparticles, namely, A5, B5, and C9 as listed in Table II. Figure 6 shows the SEM images and size distribution of prepared microparticles under these optimum conditions. The particle sizes thus obtained were 6.04 ± 0.8, 6.28 ± 1.25, and 2.23 ± 0.57 μm under the conditions A5, B5, and C9, respectively. All the prepared PLGA microparticles exhibited fairly uniform size and geometry distributions.

Table II. Optimum processing conditions.

	Test condition		
	A5	B5	C9
Voltage (kV)	9	10	11
Flow rate ratio (mL/h) core:shell	0.1 : 1	0.1 : 1	0.1 : 1
Travel distance (cm)	8	10	12
PLGA concentration (%, w/v)	6	7	7

Generally, the electrospray process includes the use of a high electric field to stretch the liquid jet at the end of the metallic tube. When the electrostatic force is high enough, the liquid forms a conical jet and finally breaks into tiny droplets. As the droplets travel to the collecting disk, the solvent evaporates. Solid particles can then be formed and collected. The experimental results in Fig. 2 suggest that the size of electrosprayed core–shell-structured PLGA microparticles decreases with increasing voltage. This is due to the fact that a higher voltage exerts a greater force in stretching the solution jet. Subsequently, the formed droplets thus exhibit a smaller particle size. The effect of core:shell solution flow rate ratio was also examined. It was found that the particle size increases with the flow rate of the shell solution (Fig. 3).

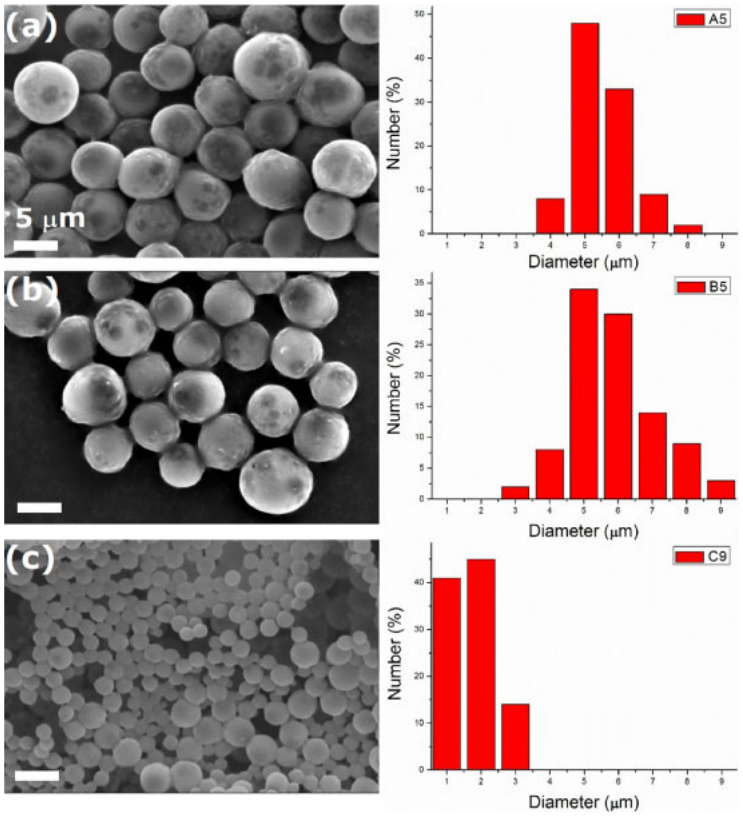

Fig. 6. (Color online) SEM images and size distribution of microparticles produced under the optimum conditions (a) A5, (b) B5, and (c) C9. Scale bar: 5 μm.

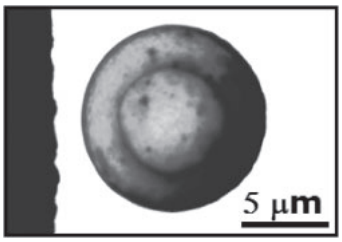

Fig. 7. TEM image of core–shell-structured microparticle (×10,000).

With the supply of a greater amount of the polymeric material in the shell solution, it becomes more difficult for the electric force to stretch the solution jet during the co-axial electrospraying process. Electrosprayed microparticles thus showed a greater size distribution. The results shown in Fig. 4 suggest that as the travel distance from the ejecting nozzle to the collecting disk is too short, the particles coagulate. This might be attributable to the fact that after being ejected out from the nozzle, the solvent evaporates as the droplet travels towards the collector. If the travel distance is not long enough, the solvents may not have enough time to completely evaporate. Sprayed microparticles may thus coagulate as shown in Fig. 4(a). Meanwhile, a longer travel distance allows the solution particles to break into smaller ones as they are subjected to the external force by the electric field. Prepared microspheres thus becomes smaller as the travel distance increases. In this study, tailed PLGA microparticles were obtained at a PLGA concentration of 8% by weight, which is the concentration that corresponds to the onset of significant chain entanglements[20,21] in the polymer [condition A9 in Fig. 5(c)]. A lower PLGA concentration may thus electrospray the solutions into microparticles with collapsed and rough surfaces [Fig. 5(a)], owing to insufficient polymeric chain entanglement.

To confirm the core–shell structure of the PLGA microparticles, TEM was employed to observe the co-axially electrosprayed particles. Core–shell-structure microparticles electrosprayed under condition B5, namely, a voltage of 10 kV, a flow rate ratio of 0.1 : 1, a travel distance of 10 cm, and a polymer concentration of 7%, were examined. The image in Fig. 7 shows the core–shell structure of an electrosprayed PLGA microparticle. Furthermore, LSCM was also utilized to verify the protein distribution in the core–shell-structured microparticle. The co-axially electrosprayed particles exhibited dispersed green signals of reGFP (Fig. 8), demonstrating a fairly homogeneous protein composition. The bioactivity of the protein was well preserved after the co-axial electrospraying process.

Finally, we found that the parameters investigated in this work affect not only the particle size distribution, but also the size ratio of the core to the shell. These should also be explored and will be the focus of our future studies.

4. Conclusions

In this study we investigated the effects of various processing parameters on the electrospraying of core–shell-structured PLGA microparticles. The size of electrosprayed core–shell particles was found to decrease with increasing voltage, travel distance, flow rate of shell solutions, and PLGA concentration in solutions. The experimental results demonstrated that under the optimum condition, core–shell-structured microparticles can be successfully prepared using a protein with high activity at the core.

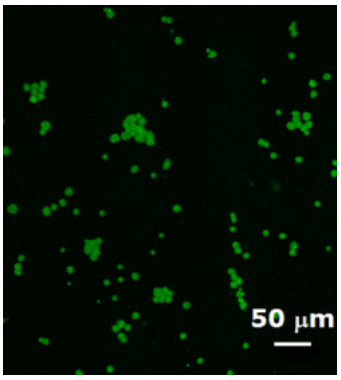

Fig. 8. (Color online) LSCM of reGFP in co-axially electrosprayed core–shell-structured particles.

Acknowledgements

The authors would like to thank the Ministry of Science and Technology, Taiwan (Contract No. 107-2221-E-182-017) and the Chang Gung Memorial Hospital (Contract No. CMRPD2H0031) for financially supporting this study.

1) S. M. Gaskell, J. Mass Spectrom. **32**, 677 (1997).
2) D. N. Nguyen, C. Clasen, and G. Van den Mooter, J. Pharm. Sci. **105**, 2601 (2016).
3) M. Enayati, M.-W. Chang, F. Bragman, M. Edirisinghe, and E. Stride, Colloids Surf. A **382**, 154 (2011).
4) N. Bock, M. A. Woodruff, D. W. Hutmacher, and T. R. Dargaville, Polymers **3**, 131 (2011).
5) S. Hao, Y. Wang, B. Wang, J. Deng, X. Liu, and J. Liu, Mater. Sci. Eng. C **33**, 4562 (2013).
6) M. P. Prabhakaran, M. Zamani, B. Felice, and S. Ramakrishna, Mater. Sci. Eng. C **56**, 66 (2015).
7) S. Hao, Y. Wang, B. Wang, J. Deng, L. Zhu, and Y. Cao, Mater. Sci. Eng. C **39**, 113 (2014).
8) K. Songsurang, N. Praphairaksit, K. Siraleartmukul, and N. Muangsin, Arch. Pharm. Res. **34**, 583 (2011).
9) S. A. Malik, W. H. Ng, J. Bowen, J. Tang, A. Gomez, A. J. Kenyon, M. Richard, and R. M. Day, J. Colloid Interface Sci. **467**, 220 (2016).
10) D. He, S. Wang, L. Lei, Z. Hou, P. Shang, X. He, and H. Nie, Chem. Eng. Sci. **125**, 108 (2015).
11) M. Zamani, M. P. Prabhakaran, E. S. Thian, and S. Ramakrishna, Int. J. Pharm. **473**, 134 (2014).
12) M. Zamani, M. P. Prabhakaran, E. S. Thian, and S. Ramakrishna, J. Colloid Interface Sci. **451**, 144 (2015).
13) P. Davoodi, F. Feng, Q. Xua, W.-C. Yan, Y. W. Tong, M. P. Srinivasan, V. K. Sharma, and C.-H. Wang, J. Control. Release **205**, 70 (2015).
14) L. Cao, J. Luo, K. Tu, L.-Q. Wang, and H. Jianga, Colloids Surf. B **115**, 212 (2014).
15) Y. Gao, D. Zhao, M.-W. Chang, Z. Ahmad, X. Li, H. Suo, and J.-S. Li, Mater. Lett. **146**, 59 (2015).
16) W. Kim and S. S. Kim, Polymer **52**, 3325 (2011).
17) Y. Wang, Y. Wei, X. Zhang, M. Xu, F. Liu, Q. Ma, Q. Cai, and X. Deng, Chem. Eng. J. **273**, 490 (2015).
18) W. Amass, A. Amass, and B. Tighe, Polym. Int. **47**, 89 (1998).
19) S. Doppalapudi, A. Jain, W. Khan, and A. J. Domb, Polym. Adv. Technol. **25**, 427 (2014).
20) N. Bhardwaj and S. C. Kundu, Biotechnol. Adv. **28**, 325 (2010).
21) A. Rogina, Appl. Surf. Sci. **296**, 221 (2014).